Semi-Physical Integration of Scattering Models for Microwaves and Optical Wavelengths

I.Baris[1,2], T. Jagdhuber[1], H. Anglberger[1], S. Erasmi[2], F. Jonard[3,4]

[1] German Aerospace Center, Microwaves and Radar Institute, P.O. Box 1116, 82234 Wessling, Germany
[2] Georg-August-University Göttingen, Institute of Geography, Cartography, GIS & Remote Sensing Dept.
[3] Forschungszentrum Jülich GmbH, Institute of Bio- and Geosciences: Agrosphere (IBG-3), 52425 Jülich, Germany
[4] Université catholique de Louvain, Earth and Life Institute, Croix du Sud 2, 1348 Louvain-la-Neuve, Belgium
E-Mail: i.baris@outlook.de, Thomas.jagdhuber@dlr.de, harald.anglberger@dlr.de, serasmi@gwdg.de, f.jonard@fz-juelich.de

***Abstract*—Various approaches exist to model scattering of a vegetation canopy above ground in terms of optical and radar wavelengths. Due to the different scattering properties these two spectral regions are modelled separately for visible/ infrared bands and for microwave regions. The newly developed RadOptics model (RO-M) integrates these two spectral regions semi-physically into one radiative transfer (RT)-based model framework, resting on the law of Beer-Bougert-Lambert. Due to the integrative nature of RO-M, it can calculate/simulate the canopy and soil reflectances for the optical and radar spectrum using a single unified model architecture. By Applying RO-M in radar domain (ROR-M) it is shown that the observed dependence of Backscattering coefficient on Leaf Area Index (LAI), soil moisture content and frequency can be simulated consistently with results in literature. The results of the RO-M within the optical domain (ROO-M) present an equivalent trend of reflectance and band ratio values with LAI compared to studies in literature.**

Keywords—modeling, physics, microwaves, optics, vegetation, soil

I. INTRODUCTION

Our planet faces several environmental challenges that will need to be solved during the 21st century. A key asset coming from the remote sensing community could be the parametrization and quantification of vegetation and soil properties for input into models and tools for decision making. Since optical sensors are useful to retrieve biophysical vitality/productivity parameters, radar sensors deliver a wide range of moisture and structure characteristics. Therefore, it is desirable to develop an integrated model on physics basis, which describes scattering characteristics in terms of both optical and radar wavelengths. With this aim, we integrated a kernel-driven optical scattering model, which provides the bidirectional reflectance (BRDF) above a horizontally homogeneous plant canopy on soil with a zeroth order radiative transfer ($\tau-\omega$) model framework [3, 4]. A semi-physical integration of different scattering kernels to form the RadOptics model (RO-M) is proposed based on the principle of gradual loss of flux intensity through a medium according to the law of Beer-Bougert-Lambert and the Radiative Transfer Theory (RT). Semi-physical means, that the sensing geometry is modeled physically and the loss of radiation due to the canopy and the surface with object specific quantities, like leaf reflectance and transmittance or soil moisture content, which is belonging to the semi-physical part. Thus, RO-M enables modeling of vegetated soils for various system and object properties/dependencies in optical and radar wavelengths like reflectance values ρ, as well as Backscatter Coefficients σ^0 (BSC), respectively.

II. INTRODUCTION TO OPTICAL SCATTERING MODELS

The later applied scattering model for optical wavelengths originates from [3, 5–7]. This kernel-driven BRDF model ρ is based on RT using the single scattering as well as geometric-optics (GO) approximations [3]:

$$\rho = \rho_{vol} + \rho_{geo} + \rho_{iso} \tag{1}$$

where ρ_{vol}, ρ_{geo} and ρ_{iso} are the volume, the geometric and the isotropic scattering contribution, respectively. As the BRDF depend only on acquisition geometry, the derived models are referred as "kernel-driven" [3]. The advantage of a kernel-driven approach is notably the analytical invertibility and the adaption to mixed pixel situations (sunlit and shadowed areas). The canopy within the RT-based model is described by its volume density N, its area A, its randomly located leaves with reflectance s and transmittance t above a flat impenetrable horizontal surface of Lambertian reflectance ρ_0. The BRDF is given by [5]

$$\rho_{vol} = \frac{w}{4NA}\frac{P(\underline{\Omega})}{\cos\theta_i\cos\theta_v}\frac{1-\exp\left\{-LAI\left[\frac{G(\theta_i)}{\cos\theta_i}+\frac{G(\theta_v)}{\cos\theta_v}\right]\right\}}{\frac{G(\theta_i)}{\cos\theta_i}+\frac{G(\theta_v)}{\cos\theta_v}} + \rho_0\exp\left\{-LAI\left[\frac{G(\theta_i)}{\cos\theta_i}+\frac{G(\theta_v)}{\cos\theta_v}\right]\right\}, \tag{2}$$

where w is the volume scattering coefficient, $G(\theta_l)$ is the foliage area orientation function, $P(\underline{\Omega})$ is the phase function of the medium and LAI is the Leaf Area Index [7, 8]. Moreover, Roujean makes in [7] the assumption that the distribution of leave orientations is random, so that w and $G(\theta_l)$ can be written as $G(\theta_l)=0.5$, where θ_l is the leaf inclination, $w = NA(s+t)/2$, and the phase function $P(\underline{\Omega})$ as described in

[5, 8]. Furthermore, Wanner [3] and Roujean [7] make the assumption $s=t$ and $0.5(\sec\theta_i+\sec\theta_v)\approx 1.5$. Adopting these assumptions and the normalization of (2) to NADIR, the equation (2) can be rewritten in kernel notation as [3, 7]

$$\rho_{vol}=\beta_{vol}k_{vol}+\alpha_{vol}\,, \tag{3}$$

where the kernel is

$$k_{vol}=\frac{\left(\frac{\pi}{2}-\xi\right)\cos\xi+\sin\xi}{\cos\theta_i+\cos\theta_v}-\frac{\pi}{4} \tag{4}$$

and the coefficients are

$$\beta_{vol}=\frac{4s}{3\pi}\left(1-\exp\{-1.5\cdot LAI\}\right), \tag{5}$$

$$\alpha_{vol}=\frac{s}{3}+\exp\{-1.5\cdot LAI\}\left(\rho_0-\frac{s}{3}\right). \tag{6}$$

The GO-based part of the optical scattering model was developed by [6]. In this approach the reflectance of a scene is modeled as an area-weighted sum of reflectances with proportion K of sunlit crown C, sunlit surface G, shaded crown T and shaded surface Z. Li assumed in [6]that the shaded areas are perfectly black $(T=Z=0)$ and sunlit ground and crown are equally bright. Accepting these assumptions, the reflection of a scene is described by

$$\rho_{geo}=C\left(K_C+K_G\right)\ . \tag{7}$$

Moreover, the BRDF from Li describes a plant canopy with a *spheroid on a stick model* to obtain the proportions K_C and K_G [6]. These spheroids are determined by their radius r, their height b_{sp} and number density of objects n [6]. With this approximation and the assumption that the number density of objects are sparse, so that one can approximate $\exp\{n\pi r^2\}\approx 1+n\pi r^2$, equation (7) can be rewritten in kernel-based notation as [3]

$$\rho_{geo}=\beta_{geo}k_{geo}+\alpha_{geo}\ , \tag{8}$$

where

$$k_{geo}=O(\underline{\Omega})-\sec\theta_i'-\sec\theta_v'+\frac{1}{2}(1+\cos\xi')\sec\theta_v' \tag{9}$$

and the coefficients are

$$\beta_{geo}=Cn\pi r^2\,, \tag{10}$$

$$\alpha_{geo}=C\,. \tag{11}$$

The other coefficients of (9), (10) and (11) are described in [3, 6]. The complete semi-physical model, which combines the RT- (3) with the GO- (8) based parts has the form

$$\rho=\rho_{vol}+\rho_{geo}+\rho_{iso}=f_{vol}k_{vol}+f_{geo}k_{geo}+f_{iso}\,, \tag{12}$$

and the coefficients are

$$f_{iso}=\delta\alpha_{geo}+(1-\delta)\alpha_{vol}\,, \tag{13}$$

$$f_{geo}=\delta\beta_{geo}\ , \tag{14}$$

$$f_{vol}=(1-\delta)\beta_{vol}\,, \tag{15}$$

where $\delta\,[0,1]$ is a weighting parameter which regulates the proportion of geometric compared to volumetric scattering [5]. The respective kernel quantities are k_{vol} (volume kernel) and k_{geo} (geometric kernel), where the factor f_{vol} and f_{geo} are respective weights of the kernel. The isotropic scattering contribution is f_{iso} [3].

III. METHODOLOGY OF NOVEL RADOPTICS MODEL

A. Semi-physical integration of RT-based models

By withdrawing the assumptions in (4), (5), (6), one will obtain the full solution of (2). First, the coefficients $G(\theta_l)$, LAI, w and ρ_0 have to be integrated. The extinction cross section in optical terms is defined as an effective particle extinction in terms of LAI, where $G(\theta_l)$ is a dimensionless geometry factor equal to the projection of a unit area of foliage. In other words, it is an attenuation factor that does not vary with wavelength, but rather with θ_l (leaf inclination). As stated in [5] one can describe the extinction coefficient in optical terms as

$$k_e=u_lG(\theta_l)\,, \tag{16}$$

where u_l is the leaf area density function. With (16) one can define the optical depth at the bottom of the canopy as [5, 9]

$$\tau=\int_0^{z_{\max}}k_e dz=\int_0^{z_{\max}}-\frac{u_lG(\theta)}{\cos\theta}dz=LAI\frac{G(\theta)}{\cos\theta} \tag{17}$$

Note, that $G(\theta_l)$ takes other types of extinction, like the extinction according to biochemical activity's e.g. photosynthesis, not into account. For this reason, one can obtain a generally form of $G(\theta_l)\sec\theta$ from (17) being a mainly angle- and phase-dependent extinction coefficient $k_e(\underline{\Omega})$ with respect to particle and biochemical extinction $k_e(\underline{\Omega})=k_e(\sec\theta_i+\sec\theta_v)$.

The next step is the integration of the volume scattering coefficient w. The authors from [3, 5, 7] proposes a simple volume scattering coefficient $w=G(\theta_l)N\sigma(s+t)$. This means, that the volume scattering depends only on $G(\theta_l)$ (projection of a unit area of foliage). Therefore, the extinction on leaf reflectance and transmittance are treated equally. According to [10] it is more advantageous to treat these extinctions separately. Thereby, under the assumption $s=t$ the new volume scattering coefficient is given by

$$w=N\sigma s\left[F_1(\theta_l)+F_2(\theta_l)\right]=N\sigma sF_{12}\,, \tag{18}$$

where F_{12} is a function of θ as well as θ_l which is multiplied by leaf reflectance to obtain volume scattering [10].

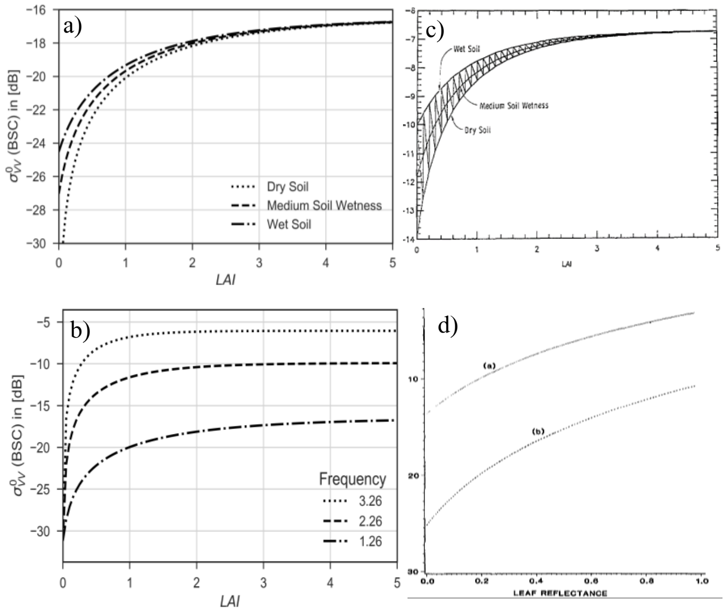

Fig. 1: σ^0 (BSC) versus LAI as calculated from RO-M for a) three different soil wetness conditions at frequency 1.26 GHz: 0.25 (wet), 0.15 (medium), 0.05 (dry), for b) three different acquisition frequencies in GHz, for c) BSC versus LAI for a corn canopy from [1], microwave frequency at 17.0 GHz, VV polarization, angle of incidence = 50° wetness conditions: 0.25 (wet), 0.15 (medium), 0.05 (dry), for d) Backscattering coefficient versus leaf reflectance from [2] to simulate frequency dependence of backscattering coefficient. Leaf angles are assumed to be uniformly distributed with an average angle of 45 °. LAI = 2.0, Soil reflectance = 0.2. Angle of incidence: (a) 20°; (b) 50 °.

Acquisition scenario for a) and b): Leaf angle = 45°, angle of incidence = 50°, scattering angle = 30°, relative azimuth angle = 50°. Weighting parameter = 0, Soil parameter: temperature = 20 °, sand and clay fraction = 0.8 and 0.15, correlation length = 28 cm, RMS height = 0.55 cm. Vegetation parameter: $k_s = 0.0038$, $k_e = 0.26$.

In the last step of the integration, the coefficient ρ_0 must be transferred into radar-equivalent terms. For optical terms the surface scattering coefficient ρ_0 describes the Lambertian reflectance of a surface (soil or surface of canopy), which is transferable to a BRDF. In radar-equivalent terms, one obtains surface scattering intensities ρ^+_{surf} like the normalized scattering coefficient σ_0 (e.g. I²EM). Moreover, the RO-M model delivers only reflectance values. Tomiyasu proposed in [11] a formal relationship between the different scattering coefficient for a diffuse surface as:

$$\sigma^0 = 4\pi \cdot \rho \cdot \cos\theta_i \cdot \cos\theta_v . \quad (19)$$

This means, the reflectance values need to be multiplied with $4\pi \cdot \cos\theta_i \cdot \cos\theta_v$ to be converted into normalized scattering coefficient σ_0.

The kernel-notation can be obtained by entering all the relationships in (2) and the phase function $P(\underline{\Omega})$ as described in [5]:

$$\rho^+_{vol} = \beta^+_{vol} K_{vol} + \alpha^+_{vol} , \quad (20)$$

where the volume scattering kernel is defined as

$$K_{vol} = \frac{\left(\frac{\pi}{2} - \xi\right)\cos\xi + \sin\xi}{\cos\theta_i + \cos\theta_v} - \frac{\pi}{4} \quad (21)$$

and the coefficients are

$$\beta^+_{vol} = \frac{2F_{12}}{3\pi}\omega\left(1 - \exp\{-\tau B\}\right), \quad (22)$$

$$\alpha_{vol} = \frac{F_{12}\omega}{3} + \exp\{-\tau B\}\left(\rho^+_{surf} - \frac{F_{12}\omega}{3}\right), \quad (23)$$

where $\tau B = dk_e\left(\sec\theta_i + \sec\theta_v\right)$ and $\omega = \frac{k_s}{k_e}$.

B. Semi-physical integration of GO-based model

Like in the section above, it is necessary to withdraw various approximations in (9), (10), (11) for the semi-physical integration. The critical term in the GO-based kernel is $n\pi r^2$ because it seems that this term has nothing to do with optical thickness. But Li and Wang presented and discussed in [12] a modified GO model, where they established a causal relationship between the term nr^2 and LAI :

$$LAI = b_{sp} \cdot nr^2 \quad (24)$$

Inserting this relationship in (8) and taking back the assumption of $\exp\{n\pi r^2\} \approx 1 + n\pi r^2$, one can obtain the geometric kernel as

$$\rho^+_{geo} = \beta^+_{geo} K_{geo} + \alpha^+_{geo} , \quad (25)$$

where the coefficients represent

$$K_{geo} = \frac{1}{2}(\cos\xi' - 1) \quad , (26)$$

$$\beta^+_{geo} = \rho^0_{vol}\left(1 - \exp\left\{\frac{-\pi\tau B'}{b_{sp} \cdot k_e}\right\}\right) , \quad (27)$$

$$\alpha^+_{geo} = \rho^+_{surf} \exp\left\{\frac{-\tau\pi\left[B' - O(\theta,\phi)\right]}{b_{sp} \cdot k_e}\right\}. \quad (28)$$

Note that ρ^0_{vol} is ρ^+_{vol} without considering a surface reflectance ($\rho^+_{surf} = 0$) and that the assumption of sunlit ground and crown are equally bright are withdrawn. Further investigations are needed to overcome the assumption that the shaded areas are perfectly black. Finally, the full semi-physical RO-model (RO-M) is represented by (12) - (15).

IV. First Modeling Results in Optical & Radar Domain

Fig. 1a visualizes the dependence of radar backscatter σ^0 (BSC in [dB]) on soil moisture content. Comparing the different soil moisture contents in Fig.2, it can be observed that as soil moisture increases, σ^0 (BSC) rises, especially for low LAI values (< 2). After comparing Fig. 2 with the literature

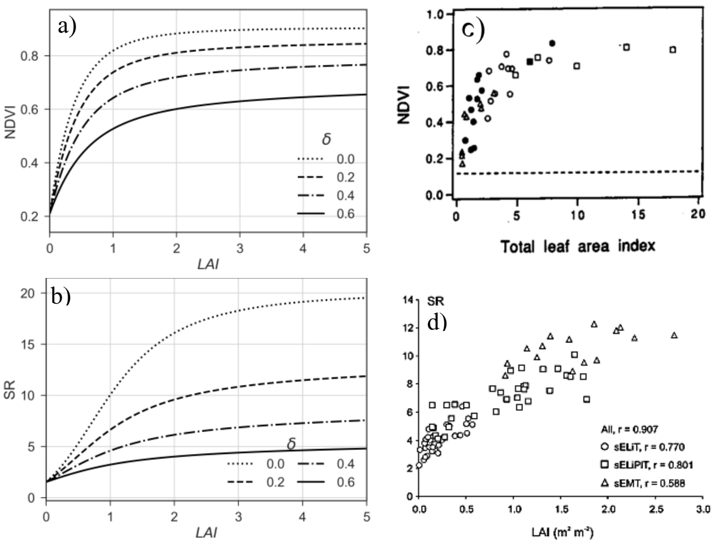

Fig. 2: NDVI and NIR-Red-Ratio (SR) versus LAI for a) and b) at different weighting parameter δ for dominance of geometric or shadowed surface over volumetric volume scattering as calculated from RO-M. Acquisition Scenario: Leaf angle = 45°, angle of incidence = 50°, scattering angle = 30°, relative azimuth angle = 50°. Band ratios calculated with PROSPECT model. Leaf structure parameter = 1. Chlorophyll a+b content = 20. Carotenoids content = 3. Brown pigments content = 0.40. Equivalent water thickness. = 0.0005. Dry matter content = 0.0085. For c) relationship between NDVI and LAI for three different California vegetation types at two different seasons from [3] and for d) relationship between LAI and ASTER SR for different mountain birch forest types from [1].

measurements from Ulaby [1] (Fig. 1c), it reveals that the simulated values of RO-M show the same dependencies in trend and scattering level.

Fig. 1b shows the dependence of σ^0 (BSC) on frequency. The reference plot from [11,12] in Fig. 1b implies that as frequency decreases, the leaves scatter less and allow more transmission of radiation which lowers σ^0 (BSC). Thus, the saturation of σ^0 (BSC) occurs at a higher value of LAI. This dependency is consistent with the field observations in [1, 13] (Fig. 1d).

The relationship between NDVI and LAI is shown in Fig. 2a. The NDVI saturates, depending on δ, approximately between 15% and 40%. The modeled NDVI indicates expected differences in a range of LAI between 0 and 2 in sparse canopy covers. The same trend and point of saturation with LAI is found in Gamon et al. [14] (see Fig. 2c).

In Fig. 2b the LAI is plotted against NIR-Red-Ratio (SR). Between LAI-values ranging around 0 and 2 the SR shows a strong linear relationship with LAI. The comparison between Fig. 4b and in situ measurements from Heiskanen [15] shows an equivalent linear relationship for LAI values between 0 and 2 (fig. 2d).

V. Acknowledgement

We are grateful to MIT for supporting this research with the MIT-Germany Seed Fund "Global Water Cycle and Environmental Monitoring using Active and Passive Satellite-based Microwave Instruments".

VI. References

[1] F. T. Ulaby, "Relating radar reflectivity to LAI," *Quart. Tech. Interchange Meeting, Nasa, Houston, TX, 1 March*, 1983.

[2] N. S. Goel, "Modeling canopy reflectance and microwave backscattering coefficient," *Remote Sensing of Environment*, vol. 18, no. 3, pp. 235–253, 1985.

[3] W. Wanner, X. Li, and A. H. Strahler, "On the derivation of kernels for kernel-driven models of bidirectional reflectance," *J. Geophys. Res.*, vol. 100, no. D10, p. 21077, 1995.

[4] T. J. Jackson and T. J. Schmugge, "Vegetation effects on the microwave emission of soils," *Remote Sensing of Environment*, vol. 36, no. 3, pp. 203–212, 1991.

[5] J. Ross, *The radiation regime and architecture of plant stands*. The Hague: Junk, 1981.

[6] X. Li and A. H. Strahler, "Geometric-Optical Bidirectional Reflectance Modeling of a Conifer Forest Canopy," *IEEE Transactions on Geoscience and Remote Sensing*, vol. GE-24, no. 6, pp. 906–919, 1986.

[7] J.-L. Roujean, M. Leroy, and P.-Y. Deschamps, "A bidirectional reflectance model of the Earth's surface for the correction of remote sensing data," *J. Geophys. Res.*, vol. 97, no. D18, p. 20455, 1992.

[8] F. T. Ulaby and C. Elachi, Eds., *Radar polarimetry for geoscience applications*. Norwood, MA: Artech House, 1990.

[9] S. Chandrasekhar, *Radiative transfer*. New York: Dover Publications, 1960.

[10] W. Verhoef, *Theory of radiative transfer models applied in optical remote sensing of vegetation canopys*. AD Emmerloord: National Aerospace Laboratory (NLR), 1998.

[11] K. Tomiyasu, "Relationship Between and Measurement of Differential Scattering Coefficient and Bidirectional Reflectance Distribution Function (BDRF)," *IEEE Transactions on Geoscience and Remote Sensing*, vol. 26, no. 5, pp. 660–665, 1988.

[12] C. Li, J. Song, and J. Wang, "Modifying Geometric-Optical Bidirectional Reflectance Model for Direct Inversion of Forest Canopy Leaf Area Index," *Remote Sensing*, vol. 7, no. 9, pp. 11083–11104, 2015.

[13] F. T. Ulaby, D. G. Long, and W. Blackwell, *Microwave radar and radiometric remote sensing*. Ann Arbor, Mich.: Univ. Of Michigan Press, 2014.

[14] J. A. Gamon *et al.,* "Relationships Between NDVI, Canopy Structure, and Photosynthesis in Three Californian Vegetation Types," *Ecological Applications*, vol. 5, no. 1, pp. 28–41, 1995.

[15] J. Heiskanen, "Estimating aboveground tree biomass and leaf area index in a mountain birch forest using ASTER satellite data," *International Journal of Remote Sensing*, vol. 27, no. 6, pp. 1135–1158, 2006.